MRS Advances © 2017 Materials Research Society
DOI: 10.1557/adv.2017.466

Fabrication of Thin Metal-Organic Framework MOF Films on Metal-Ion-crosslinked GO-modified Supports

Julius Choi[1], Hyuk Taek Kwon[2], and Hae-Kwon Jeong*[2,3]
[1]Department of Biological and Agricultural Engineering, Texas A&M University, College Station, TX 77843-2117, United States.
[2]Artie McFerrin Department of Chemical Engineering and [3]Department of Materials Science and Engineering, Texas A&M University, College Station, TX 77843-3122, United States.
* Corresponding author, email address: hjjeong7@tamu.edu

ABSTRACT

Thin films of metal-organic frameworks (MOFs) have shown promising for applications such as gas separation, gas storage, optoelectronics or sensing. However, synthesis of polycrystalline MOF films and membranes depends largely on the surface properties of supports, limiting the availability of common supports. It is, therefore, highly desirable to develop ways to modify the surface properties of common supports for the preferred heterogeneous nucleation of the MOFs. Here, we demonstrated that graphene-oxide (GO) can be exploited to readily modify the surface properties of common supports, thereby leading to well inter-grown polycrystalline MOF films. A prototypical zeolitic-imidazolate framework ZIF-8 was chosen as a model MOF system. The stabilization of GO layers with divalent metal ions was found a key step to synthesize well inter-grown ZIF-8 films. The effect of divalent metal ions on the stability of GO layers and the quality of the resulting ZIF-8 films were systematically investigated. Finally, the single gas permeation behaviors of the ZIF-8 films grown on GO-modified supports were tested.

INTRODUCTION

Metal-organic frameworks (MOFs), a new class of crystalline nanoporous materials formed by the assembly of metal ions and organic ligands, have attracted a great deal of interest primarily due to their exceptionally high surface areas/pore volumes as well as tunable pores/cavities with a judicious choice of organic linkers [1]. In particular, zeolitic-imidazolate frameworks (ZIFs), a subclass of MOFs, consisting of zinc or cobalt metal centers and imidazolate-derived linkers, have attracted tremendous attentions due to their relatively high chemical/thermal stabilities, their ultra-microporosities, and high surface area when compared to other MOF materials [2]. For example, thin films of a prototypical ZIF-8 constructed from zinc and 2-methylimidzolate have shown great promises as high-performance sensors and highly selective membranes [1,2].

The applications of MOF materials such as in optical, sensing, and membrane-based separation applications often require the facile formation of MOF thin films on supports of choice [1,3]. However, synthesis of polycrystalline MOF films on supports (either porous or nonporous) requires preferential nucleation of MOF crystals on supports. As such, there are only a handful of supports used for continuous polycrystalline MOF films and membranes including a few oxides and polymers [1-4]. One strategy to improve the heterogeneous nucleation of MOFs on supports is to modify supports with thin layers of polymeric materials containing MOF nucleation-friendly functional groups such as polyethyleneamine (PEI) [5-7]. The polymer-modified supports, however, might not be desirable if applications require relatively harsh

conditions since most polymers exhibit relatively poor thermal/mechanical/chemical properties. It is, therefore, highly desirable to find thermally/mechanically/chemically robust materials that can be easily applied and modify supports such that the heterogeneous nucleation of MOF materials is enhanced, resulting in the facile formation of polycrystalline MOF films.

Graphene oxides (GO) are atom-thick sheets of carbon possessing many oxygen-containing functional groups such as carboxylic, epoxy, and hydroxyl groups. GO dispersion can be readily used for the preparation of thin films, papers, or membranes with various thicknesses in controlled manners [8-10]. These GO films exhibit outstanding mechanical/chemical/thermal properties as well as good flexibility [8-10]. Besides, owing to their oxygen functional groups, GOs can be readily used as a component for composite materials including GO/MOF composite particles, including GO/HKUST-1, GO/ZIF-8, GO/MOF-5 and GO/MIL-101 [11]. These studies strongly suggest that thin GO layers can modify substrates to promote heterogeneous nucleation of MOF crystal growth as more stable modifying layer as compared to polymer layers. Interestingly, Wang and his coworkers [12] reported the preparation of ultra-thin ZIF-8/GO nanocomposite membranes. They first prepared hybrid GO nanosheets where a suitable number of ZIF-8 nanoparticles crystallized on the surface of GO nanosheets. Then they deposited the hybrid GO nanosheets on anodized aluminum oxide (AAO) supports and subsequently grew ZIF-8 nanocrystals on GO nanosheets into continuous films.

Here, we investigate ultra-thin GO layers to modify supports for facile preparation of MOF films using ZIF-8 as a model MOF system. It was found essential that GO layers needed to be stabilized since as-prepared GO layers readily underwent disintegration under the growth conditions. It turned out that soaking as-prepared GO layers in metal ion solutions was an effective way to stabilize GO layers via electrostatic interactions. In addition, Zn^{2+} and Co^{2+} were found to be most effective in stabilizing GO layers as well as in forming well inter-grown ZIF-8 films. Finally, the gas permeation performances of these ZIF-8 films were determined.

EXPERIMENT

Chemicals

Zinc nitrate hexahydrate ($Zn(NO_3)_2 \cdot 6H_2O$, 98%, Sigma-Aldrich), cobalt nitrate hexahydrate ($Co(NO_3)_2 \cdot 6H_2O$, 98%, Sigma-Aldrich), cupric nitrate hexahydrate ($Cu(NO_3)_2 \cdot 6H_2O$, 99%, Sigma-Aldrich) and iron chloride ($FeCl_2$, 97%, Sigma-Aldrich) were used as metal sources. 2-methylimidazole ($C_4H_6N_2$, 99%, Sigma-Aldrich) was used as an organic ligand. Deionized water and ethanol (99.5%, Alfa Aesar) were solvents. Graphene oxide (300 – 800 nm) was purchased from Cheap tube. Methyl cellulose ester (MCE) filter (250 nm, Millipore) was used.

Preparation of α-Al_2O_3 supports

Porous α-Al_2O_3 supports were prepared following a previously reported protocol [13]. 1.9 g of alumina powder (CR6, Baikowski) was mixed with 8 mg of polyvinyl alcohol (PVA) solution (binder) and grinded in mortar to eliminate aggregated powder. Then the powder was injected into a die and compressed uniaxial with 10 ton for 1 min. The molded disks were sintered at 1100 °C for 2 h. The disks were polished with a sand paper (grid #1200) and washed with methanol under sonication for 1min. Finally, the disks were dried at 120 °C in an oven before usage. The prepared disks have a dimension of 22 mm in diameter and 2 mm in thickness with 46% of porosity.

Preparation of the metal ion cross-linked GO films on α-Al_2O_3 supports

An aqueous dispersion of GO solution (0.05mg/ml) was prepared and slip-coated onto homemade α-Al_2O_3 disks. The GO layers were dried in a convection oven at 60 °C for 6 h. The GO layers were then soaked in 0.01M metal ion (Zn^{2+}, Co^{2+}, Cu^{2+} and Fe^{2+}) solutions for 6 h followed by drying in a convection oven at 60 °C for 6 h

Fabrication of ZIF-8 films on GO-modified supports

ZIF-8 films were prepared using the recipe reported by Pan et al [14]. A ligand solution was prepared by dissolving 2.27g of 2-methylimidazolte (hereafter mIm) in 20 ml of water under stirring for 10 minutes. Similarly, a zinc solution was prepared by dissolving 0.11g of zinc nitrate in 20 ml water under stirring for 10 min. The two solutions were then mixed and kept stirred for 1 minutes. Cross-linked GO films were then placed vertically in the precursor solution and left for 12 h at room temperatures. Samples then were washed using a copious amount of methanol under stirring for 1 h and dried in a convection oven for 12 h at 60 °C.

Stability test of the metal ion cross-linked GO films

GO films were prepared on MCE filter paper through a vacuum filtration using 2 ml of aqueous GO solution (2 mg/ml)**.** Prepared GO films were dried in a convection oven for 12 h at 60 °C. GO films were then soaked in 0.1M metal ion (Zn^{2+}, Co^{2+}, Cu^{2+} and Fe^{2+}) solutions for 12 h followed by drying in a convection oven at 60 °C for 12 h. As-prepared GO films and the metal ion cross-linked GO films were sonicated using a bath sonication as a function of time (10, 20, 40, 60 and 120 sec). In order to collect the aqueous dispersion of detached GO sheets, samples were centrifuged for 10 min at 8000 rpm. The UV absorption of supernatants was measured at 230 nm.

Characterizations

Crystal phase was identified using a Rigaku MiniFlex II powder X-ray diffractometer with Cu-Kα radiation (λ=1.5406Å). JEOL JSM-7500F was employed to obtain electron micrographs of samples. For mechanical and structural stability tests, a bath sonicator (model-150D, VWR scientific) was used. A UV spectrophotometer (UV-1500, Shimidazu) was used for the measurement of UV absorption. Single gas permeation measurements were performed for H_2, N_2, O_2, CH_4, CO_2, C_3H_6, and C_3H_8 through ZIF-8 films on GO-modified supports through a time lag method [15] at room temperature and a feed pressure of 1 bar.

RESULTS AND DISCUSSION

Stabilization of GO films and the fabrication of ZIF-8 films on GO-modified supports

Figure 1 presents the schematic illustration of the synthesis of MOF films on GO-modified supports. ZIF-8 was chosen as a model MOF due to the simplicity of its synthesis and its potential for practical applications. ZIF-8 can be synthesized in several different solvents such as methanol, water and dimethylformide (DMF) [2]. In water, the functional groups of GO nanosheets are expected more readily deprotonated than in methanol and DMF [16, 17]. Therefore, more nucleation sites on GO nanosheets may be formed in water, resulting in well inter-grown ZIF-8 films. Besides, ZIF-8 membranes prepared in an aqueous precursor solution showed outstanding gas separation performance [14]. In light of the above-mentioned considerations, aqueous recipe was chosen for the current studies. As illustrated in Figure 1, GO-

modified supports were prepared by slip-coating an aqueous dispersion of GO nanosheets on alumina supports. However, as-prepared GO layers turned out not stable in the aqueous precursor solutions. This is primarily due to the electrostatic repulsion between charged functional groups of GO nanosheets [18-20]. It was, therefore, essential to stabilize the GO layers in order to synthesize high quality ZIF-8 films on GO-modified supports.

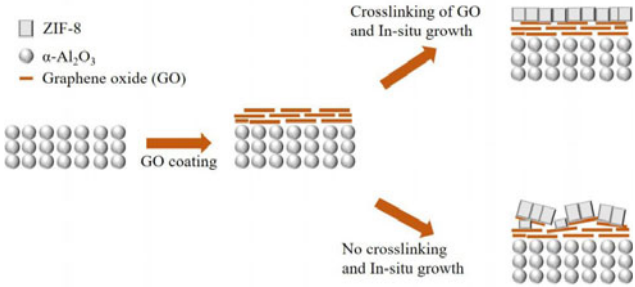

Figure 1. A schematic illustration of the fabrication of ZIF-8 films on GO-modified supports. As-prepared GO layers led to defective ZIF-8 films while cross-linked GO layers resulted in well inter-grown ZIF-8 films.

Yeh et al. [19] reported that divalent metal ions such as Zn^{2+}, Co^{2+}, and Cu^{2+} could stabilize GO layers by crosslinking GO layers through the electrostatic interactions between positively charged metal ions and negatively charged functional groups on GO nanosheets. Based on this, as-prepared GO layers were submerged in the aqueous solutions of Zn^{2+} ions, expecting that Zn^{2+} ions not only stabilize GO layers but also further promote nucleation and growth of ZIF-8 crystals since Zn^{2+} is the metal component of ZIF-8. To test the stabilizing effects of zinc ions, GO-modified supports with and without crosslinking the top GO layers via zinc ions (hereafter, G-Zn and G, respectively). As can been in Figure 2, G-Zn layer preserved even after submerged in water for 12 h while as-prepared G layer was disintegrated.

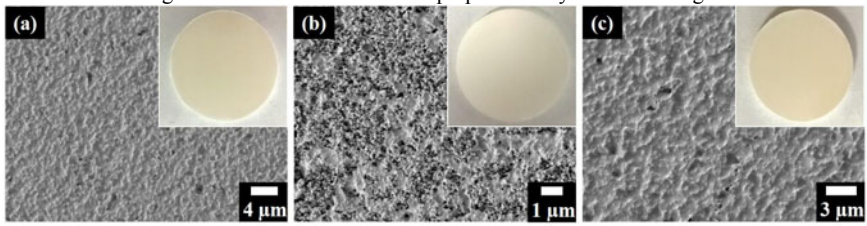

Figure 2. SEM images and optical micrographs (inset) of (a) as-prepared GO layer, (b) G layer in water for 12 h, and (c) G-Zn layer in water for 12 h.

Figure 3a shows the X-ray diffraction patterns of ZIF-8 films prepared on supports modified with Zn^{2+}-crosslinked GO and uncross-linked GO layers (hereafter, G-Zn-ZIF-8 and G-ZIF-8, respectively). Both films exhibit phase pure ZIF-8 crystals formed on the supports. The {110} peak of G-Zn-ZIF-8 film noticeably smaller as compared to that of G-ZIF-8 while the intensities of the rest of the peaks are similar. This indicates that ZIF-8 crystals formed on

crosslinked GO layers exhibit slightly more oriented perpendicular to the support. SEM images of G-ZIF-8 film (Figure 3b and 3c) show poorly inter-grown with a significant portion of the film detached from the support. In contrast, well inter- grown ZIF-8 films were formed on the support modified with Zn^{2+}-crosslinked GO layers as shown in Figure 3d and 3e. As can be seen in the figure, the thickness of the G-Zn-ZIF-8 film is ~ 1 μm with the grain size of ~ 0.5 μm. It should be noted here that the G-Zn-ZIF-8 film is one of the thinnest ZIF-8 films reported. As compared with G-ZIF-8 film, the smaller grain size as well as the smaller thickness of G-Zn-ZIF-8 film strongly suggest that the heterogeneous nucleation of ZIF-8 is greatly enhanced by the presence of zinc ions on the crosslinked GO layers.

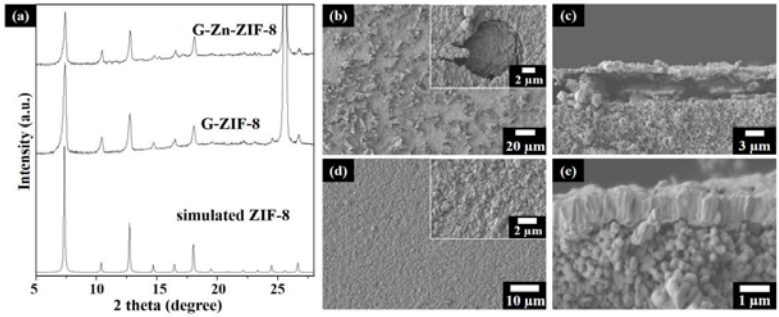

Figure 3. (a) XRD patterns of G-ZIF-8 and G-Zn-ZIF-8 and SEM images of (b,c) G-ZIF-8 and (d,e) G-Zn-ZIF-8.

Effect of nature of GO-crosslinking divalent metal ions on ZIF-8 films

It is hypothesized that the quality of ZIF-8 films may depend on the nature of metal ions crosslinking GO layers. In order to test this hypothesis, we first performed the water stability test of GO layers crosslinked with three additional divalent ions, Co^{2+}, Cu^{2+}, and Fe^{2+} (G-Co, G-Cu, and G-Fe, respectively). Figure 4 displays the UV absorbance at 230 nm of the aqueous dispersions of GO nanosheets detached from GO, G-Zn, G-Co, G-Cu, and G-Fe layers as functions of sonication time. As can be seen, all of these divalent ions appear effective in stabilizing GO layers. There were, however, less GO nanosheets detached from G-Cu and G-Fe than G-Co and G-Zn. This indicates that Cu^{2+} and Fe^{2+} are more effective stabilizing GO layers than Zn^{2+} and Co^{2+}.

ZIF-8 films were grown on alumina supports modified with GO layers crosslinked with above tested divalent metal ions. XRD patterns presented in Figure 5a indicate that phase-pure ZIF-8 films were formed regardless of crosslinking metal ions. As can be seen in the SEM images (Figure 5b-e), the surface morphologies of these ZIF-8 films were drastically different. G-Zn and G-Co-ZIF-8 films were well inter-grown and free of defects while G-Cu-ZIF-8 film showed not as well inter-grown. On the contrary, G-Fe-ZIF-8 film showed macroscopic defects with well inter-grown domains. It is our hypothesis that the kinetics of ion-exchange process and consequent change in the interaction strength between GO nanosheets and metal ions during the crystallization reaction might be responsible for the formation of defects [21, 22]. For example, with the most defective G-Fe-ZIF-8 sample, during the crystallization reaction, ion-exchange reaction of Fe^{2+} in the GO layer with Zn^{2+} is expected to happen, driven by the contra-diffusion of Fe^{2+} and Zn^{2+} between the G-Fe layer and the growth solution. During this ion-exchange

process, the GO layers might undergo partial disintegration since Fe^{2+} cannot be incorporated in the formation of ZIF-8, leading to the formation of defects. However, in the case of both G-Zn and G-Co layers, despite the presence of ion diffusion, both Zn^{2+} and Co^{2+} can be incorporated to the structure of ZIF-8 crystals (Co-substituted ZIF-8 is formally known ZIF-67 [23]), thereby forming ZIF-8 crystals as ion exchange. In the case of G-Cu-ZIF-8 film, it is noted that Cu^{2+} can be partially incorporated into the ZIF-8 framework [24], thereby resulting in continuous ZIF-8 film despite some defects. The G-Co-ZIF-8 film possesses considerably smaller grains as compared to the G-Zn-ZIF-8 film. This is likely due to the fact that the nucleation rate of Co-ZIF-8 is much faster than that of Zn-ZIF-8 as reported by Hillman et al [25].

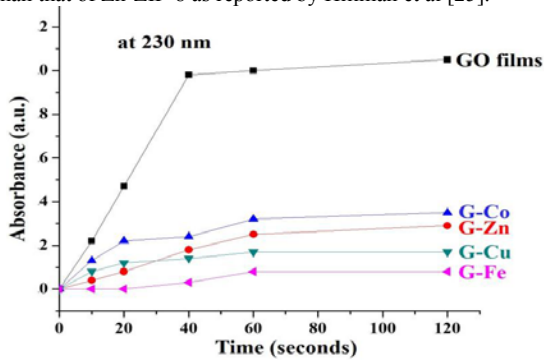

Figure 4. UV absorption of the aqueous dispersion of GOs detached from GO, G-Zn, G-Co, G-Cu, and G-Fe layers after sonication for different time.

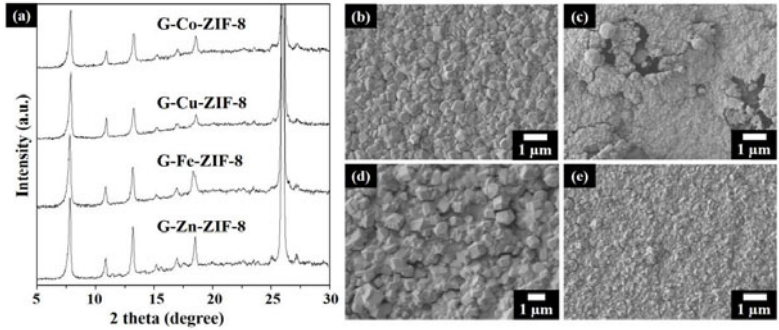

Figure 5. (a) XRD patterns of G-Zn-ZIF-8, G-Fe-ZIF-8, G-Cu-ZIF-8, and G-Co-ZIF-8 films and SEM images of (b) G-Zn-ZIF-8, (c) G-Fe-ZIF-8 and (d) G-Cu-ZIF-8, and (e) G-Co-ZIF-8 films.

Single gas permeation behaviors of G-Zn-ZIF-8 films

Finally, we investigated the single gas permeation behaviors of G-Zn and G-Zn-ZIF-8 films. As seen in Figure. 6, both films showed the selectivity toward hydrogen molecules. The reduction in the single gas permeances through the G-Zn-ZIF-8 film was observed compared to G-Zn films, suggesting that ZIF-8 films were well inter-grown. Both films show similar ideal

selectivities for H_2/CO_2, H_2/N_2, and H_2/CH_4 while G-Zn-ZIF-8 film exhibits somewhat higher H_2/C_3H_6 and H_2/C_3H_8 ideal selectivities than G-Zn film (see Figure 6b), primarily due to the limited aperture of ZIF-8 for larger molecules such as C3 hydrocarbons. However, the ideal selectivities of H_2/C_3H_6 and H_2/C_3H_8 of G-Zn-ZIF-8 film is much lower than those of ZIF-8 membranes reported[14]. This suggests that ZIF-8 films on alumina supports modified with Zn^{2+}-crosslinked GO layers exhibit relatively poor grain boundary structure. Further studies are necessary to improve the grain boundary structure of G-Zn-ZIF-8 membranes.

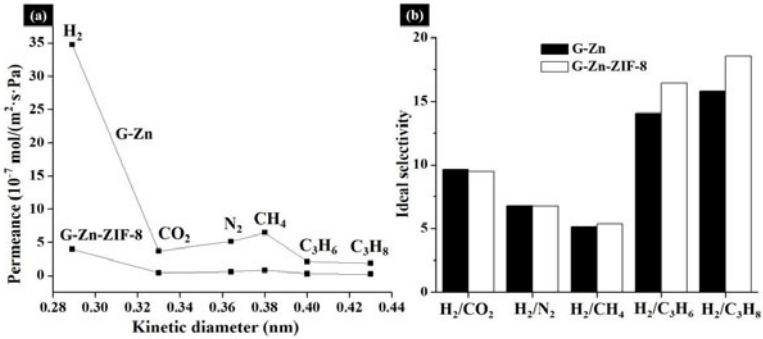

Figure 6. (a) Single gas permeances and (b) ideal selectivities of G-Zn and G-Zn-ZIF-8 films

CONCLUSIONS

Here, we explored ultra-thin GO layers as an effective, yet potentially general interlayer material to modify supports of choice for the facile fabrication of high quality MOF films. It was of critical importance to be able to stabilize GO layers by cross-linking GO nanosheets with divalent metal ions. The effect of the cross-linking divalent metal ions was systematically investigated, revealing that Co^{2+} and Zn^{2+} were most effective for the synthesis of well inter-grown ZIF-8 films. This is attributed to the fact that both of these ions can be readily incorporated into the framework of ZIF-8. This suggests that it is critical to stabilize modifying GO layers with metal ions that are components of growing MOFs. G-Zn and G-Zn-ZIF-8 films showed the selective permeation towards hydrogen. The C3 separation performance of G-Zn-ZIF-8 film was not impressive, likely due to its poor grain boundary structure.

ACKNOWLEDGMENTS

J.C. appreciates the financial support from the Mary Kay O'Connor Process Safety Center at Texas A&M University. H.-K.J. acknowledges the financial support from the National Science Foundation (CBET-150530) and in part from the Qatar National Research Fund (NPRP 7-042-2-021 and NPRP 8-001-2-001). The FE-SEM acquisition was supported by the National Science Foundation under Grant DBI-0116835, the VP for Research Office, and the Texas A&M Engineering Experimental Station.

REFERENCES

1. S. Qiu, M. Xue and G. Zhu, Chemical Society Reviews **43** (16), 6116-6140 (2014).
2. J. Yao and H. Wang, Chemical Society Reviews **43** (13), 4470-4493 (2014).
3. O. Shekhah, J. Liu, R. A. Fischer and C. Woll, Chemical Society Reviews **40** (2), 1081-1106 (2011).
4. D. Bradshaw, A. Garai and J. Huo, Chemical Society Reviews **41** (6), 2344-2381 (2012).
5. R. Ranjan and M. Tsapatsis, Chemistry of Materials **21** (20), 4920-4924 (2009).
6. M. d. M. Darder, S. Salehinia, J. B. Parra, J. M. Herrero-Martinez, F. Svec, V. Cerdà, G. Turnes Palomino and F. Maya, ACS Applied Materials & Interfaces **9** (2), 1728-1736 (2017).
7. Y. Zhang, X. Feng, S. Yuan, J. Zhou and B. Wang, Inorganic Chemistry Frontiers **3** (7), 896-909 (2016).
8. G. Eda and M. Chhowalla, Advanced Materials **22** (22), 2392-2415 (2010).
9. J. W. Suk, R. D. Piner, J. An and R. S. Ruoff, ACS Nano **4** (11), 6557-6564 (2010).
10. D. A. Dikin, S. Stankovich, E. J. Zimney, R. D. Piner, G. H. B. Dommett, G. Evmenenko, S. T. Nguyen and R. S. Ruoff, Nature **448** (7152), 457-460 (2007).
11. I. Ahmed and S. H. Jhung, Materials Today **17** (3), 136-146 (2014).
12. Y. Hu, J. Wei, Y. Liang, H. Zhang, X. Zhang, W. Shen and H. Wang, Angewandte Chemie International Edition **55** (6), 2048-2052 (2016).
13. H. T. Kwon and H.-K. Jeong, Journal of the American Chemical Society **135** (29), 10763-10768 (2013).
14. Y. Pan, T. Li, G. Lestari and Z. Lai, Journal of Membrane Science **390–391** (0), 93-98 (2012).
15. M. Shah, H. T. Kwon, V. Tran, S. Sachdeva and H.-K. Jeong, Microporous and Mesoporous Materials **165**, 63-69 (2013).
16. J. I. Paredes, S. Villar-Rodil, A. Martínez-Alonso and J. M. D. Tascón, Langmuir **24** (19), 10560-10564 (2008).
17. D. Li, M. B. Muller, S. Gilje, R. B. Kaner and G. G. Wallace, Nat Nano **3** (2), 101-105 (2008).
18. H. Huang, Y. Ying and X. Peng, Journal of Materials Chemistry A **2** (34), 13772-13782 (2014).
19. C.-N. Yeh, K. Raidongia, J. Shao, Q.-H. Yang and J. Huang, Nat Chem **7** (2), 166-170 (2015).
20. O. C. Compton, S. W. Cranford, K. W. Putz, Z. An, L. C. Brinson, M. J. Buehler and S. T. Nguyen, ACS Nano **6** (3), 2008-2019 (2011).
21. B. Zawisza, R. Sitko, E. Malicka and E. Talik, Analytical Methods **5** (22), 6425-6430 (2013).
22. G. Zhao, J. Li, X. Ren, C. Chen and X. Wang, Environmental Science & Technology **45** (24), 10454-10462 (2011).
23. H. T. Kwon, H.-K. Jeong, A. S. Lee, H. S. An and J. S. Lee, Journal of the American Chemical Society **137** (38), 12304-12311 (2015).
24. A. Schejn, A. Aboulaich, L. Balan, V. Falk, J. Lalevee, G. Medjahdi, L. Aranda, K. Mozet and R. Schneider, Catalysis Science & Technology **5** (3), 1829-1839 (2015).
25. F. Hillman, J. M. Zimmerman, S.-M. Paek, M. R. A. Hamid, W. T. Lim and H.-K. Jeong, Journal of Materials Chemistry A **5** (13), 6090-6099 (2017).